Icariside II protects dopaminergic neurons from 1-methyl-4-phenylpyridinium-induced neurotoxicity by downregulating HDAC2 to restore mitochondrial function

WENBO FAN[1] and JIANWU ZHOU[2]

[1]Pharmaceutical Technology Department, Chemical Engineering School, Jiuquan Vocational Technical College, Jiuquan, Gansu 735000; [2]Medical Laboratory of Qinghai Provincial People's Hospital, Xining, Qinghai 810000, P.R. China

Received February 28, 2023; Accepted August 18, 2023

DOI: 10.3892/etm.2023.12328

Abstract. Parkinson's disease (PD) is the second most common neurodegenerative disease after Alzheimer's disease (AD). Icariside II (ICS II) is known to confer notable therapeutic effects against a variety of neurodegenerative diseases, such as AD. Therefore, the present study aimed to evaluate the possible effects of ICS II on 1-methyl-4-phenylpyridinium (MPP^+)-induced SK-N-SH cell injury, in addition to understanding the underlying mechanism of action. The MPP^+-induced SK-N-SH cell model was used to simulate PD *in vitro*. The viability and mitochondrial membrane potential of SK-N-SH cells were detected by MTT assay and JC-1 staining, respectively. Lactate dehydrogenase (LDH) release, ATP levels and complex I activity in treated SK-N-SH cells were measured using LDH activity, ATP and Complex I assay kits, respectively. The protein expression levels of histone deacetylase 2 (HDAC2) and γ-H2A histone family member X and the copy number of mitochondrial DNA were measured by western blotting or reverse transcription-quantitative PCR, respectively. Autodock 4.2 was used to predict the molecular docking site of ICS II on HDAC2. The results of the present study demonstrated that ICS II mitigated SK-N-SH cytotoxicity induced by MPP^+. Specifically, ICS II alleviated DNA damage and restored mitochondrial function in SK-N-SH cells treated with MPP^+. In addition, ICS II reduced the HDAC2 protein expression levels in MPP^+-induced SK-N-SH cells. However, overexpression of HDAC2 reversed the protective effects of ICS II on DNA damage and mitochondrial dysfunction in MPP^+-induced SK-N-SH cells. In conclusion, the results of the present study suggest that ICS II can protect dopaminergic neurons from MPP^+-induced neurotoxicity by downregulating HDAC2 expression to restore mitochondrial function.

Correspondence to: Dr Jianwu Zhou, Medical Laboratory of Qinghai Provincial People's Hospital, 2 Gonghe Road, Xining, Qinghai 810000, P.R. China
E-mail: zhoujianwu910112@163.com

Key words: icariside II, dopaminergic neurons, neurotoxicity, histone deacetylase 2, mitochondrial function

Introduction

Parkinson's disease (PD) is a degenerative neurological disorder that is prevalent worldwide, affecting 3.7% individuals aged >65 years (1). At present, the prevalence rate of PD is high and 7-10 million individuals worldwide are reported to suffer from PD (2). PD has a chronic course, involving main pathological features including dopamine deficiency and degeneration of substantia nigra dopamine neurons (3). In addition, PD is characterized by a high disability rate, impairing the performance of daily activities, which are mediated by dopamine. Therefore, understanding the pathogenesis of PD and the development of effective drug treatments are important for improving the quality of life of patients with PD whilst reducing the disease burden on society.

Icariside II (ICS II; Fig. 1A) is an active flavonoid that can be extracted from the Chinese herb *Epimedium*, which has been shown to inhibit the inflammatory response and microcirculation disturbance, and reduce the damage caused by vascular dementia (4). In addition, ICS II has been reported to show protective activity in the central nervous system (5,6). ICS II can confer therapeutic effects against certain neurodegenerative diseases, such as Alzheimer's disease (AD) (7-10). In a model of streptozotocin-induced rats with AD, ICS II treatment was found to increase the survival of hippocampal neurons and inhibit neuroinflammation (7). Furthermore, ICS II has been demonstrated to inhibit neuronal apoptosis and neuroinflammation in amyloid β-peptide 25-35-induced AD rats (8). ICS II has also been observed to improve neurogenesis and inhibit mitochondrial division, contributing to cognitive recovery in AD mice (9). In another previous study, ICS II was shown to improve spatial learning and memory impairment in AD mice (10). However, to the best of our knowledge, the potential effects of ICS II on PD remain unclear.

Histone deacetylases (HDACs) have previously been reported to be epigenetic targets for treating PD (11). HDAC2 is a class I HDAC that has been reported to serve an important role in chromosome structure modification and gene expression regulation (12). Histone deacetylation facilitates the binding

of DNA to the histone octamer, which stabilizes the nucleosome structure and prevents the specific binding of certain transcription factors to DNA binding sites, in turn inhibiting gene expression (13,14). Previous studies have reported that HDAC2 inhibition can prevent the loss of microglial cells and dopaminergic neurons in the substantia nigra in PD (15,16).

1-methyl-4-phenylpyridinium (MPP^+) is the neurotoxic form of methyl-4-phenyl-1,2,3,6-tetrahydropyridine (mPTP). MPP^+ can been taken up by dopaminergic neurons, leading to mitochondrial dysfunction, oxidative stress and programmed cell death, which simulates the parkinsonian syndrome in cell and animal models (17). In the present study, the 1-methyl-4-phenylpyridinium (MPP^+)-induced SK-N-SH cell model was used to simulate PD *in vitro*. The present study aimed to evaluate the potential effects of ICS II on MPP^+-induced SK-N-SH cell injury, in addition to understanding the underlying mechanism of action.

Materials and methods

Bioinformatics tools. A search of the SuperPreD database (https://prediction.charite.de/subpages/target_prediction.php) demonstrated that both HDAC2 and HDAC8 were potential targets for ICS II. Based on a relatively high value of 'Model accuracy' (93.99 and 94.75% for HDAC8 and HDAC2, respectively), HDAC2 was selected for further investigation in the present study.

Cell culture and treatment. The human neuroblastoma cell line SK-N-SH (cat. no. CL-0214) was purchased from Procell Life Science & Technology Co., Ltd. SK-N-SH cells were cultured in DMEM (HyClone; Cytiva) supplemented with 10% FBS (Thermo Fisher Scientific, Inc.) and 1% penicillin/streptomycin mixture (Thermo Fisher Scientific, Inc.) at 37˚C with 5% CO_2.

SK-N-SH cells were pre-treated with 2 mM MPP^+ (MilliporeSigma) for 24 h at 37˚C to establish the *in vitro* PD cell model (18). MPP^+-induced and untreated control SK-N-SH cells were treated with different concentrations of ICS II (0, 12.5, 25 and 50 μM; MilliporeSigma) for 24 h at 37˚C (19).

MTT assay. After the aforementioned cell treatments, SK-N-SH cells were seeded into a 96-well plate at a density of $1x10^3$ cells/well and cultured for 24 h at 37˚C. SK-N-SH cells were then incubated with 10 μl 5 mg/ml MTT reagent (MilliporeSigma) for 4 h at 37˚C. After removing the culture supernatant, SK-N-SH cells were incubated with 250 μl DMSO for 20 min at room temperature to dissolve the formazan crystals. The absorbance at a 570 nm wavelength was detected using a microplate reader.

Cell transfection. HDAC2 (NC_000006.12) was cloned into the pcDNA3.1 vector to obtain HDAC2-overexpression (Oe-HDAC2) vector (Guangzhou Ruibio Co., Ltd.) and the empty pcDNA3.1 vector was used as a negative control (Oe-NC). SK-N-SH cells were transiently transfected with 1 μg Oe-NC or 1 μg Oe-HDAC2 for 48 h at 37˚C using Lipofectamine® 2000 (Thermo Fisher Scientific, Inc.) in accordance with the manufacturer's instructions. At 48 h post-transfection, subsequent experiments were conducted.

Immunofluorescence. After the aforementioned treatments, SK-N-SH cells cultured in 24-well plates at a density of $5x10^4$ cells/well were fixed with 4% paraformaldehyde at 4˚C for 15 min and incubated in 0.1% Triton X-100 in PBS for 15 min at 37˚C. After blocking with 10% BSA (Gold Biotechnology) for 1 h at room temperature, SK-N-SH cells were incubated with a primary antibody against 8-hydroxydesoxyguanosin (8-OHdG; cat. no. sc-393871; 1:100 dilution; Santa Cruz Biotechnology, Inc.) overnight at 4˚C. The cells were then incubated with FITC-conjugated goat anti-mouse secondary antibodies (cat. no. ab6785; 1:1,000 dilution; Abcam) for 1 h at room temperature. SK-N-SH cell nuclei were stained with 1 μg/ml DAPI (MilliporeSigma) for 30 min at room temperature, before being imaged using a fluorescence microscope (Olympus Corp.).

Western blot analysis. After the aforementioned treatments, SK-N-SH cells were lysed using RIPA lysis buffer (Hunan Auragene Biotech Co., Ltd.), before being centrifuged for 10 min at 10,000 x g at 4˚C to obtain total proteins. The concentration of total proteins was measured using a BCA assay kit (Beyotime Institute of Biotechnology). The protein samples (30 μg per lane) were subjected to 10% SDS-PAGE before being transferred onto PVDF membranes (MilliporeSigma). After blocking with 5% skimmed milk for 1 h at room temperature, membranes were incubated with primary antibodies against γ-H2A histone family member X (γ-H2AX; 1:5,000 dilution; cat. no. ab81299; Abcam), HDAC2 (1:2,000 dilution; cat. no. ab32117; Abcam) and GAPDH (1:2,500 dilution; cat. no. ab9485; Abcam) overnight at 4˚C. The next day, after washing using TBS-0.1% Tween-20, membranes were incubated with goat anti-rabbit HRP-conjugated secondary antibodies (1:3,000 dilution; cat. no. ab6721; Abcam) for 1 h at room temperature. Protein bands were visualized using an Immobilon Western HRP Substrate (MilliporeSigma). The band intensity of proteins was semi-quantified using the ImageJ software (version 1.49; National Institutes of Health).

JC-1 staining. After the aforementioned cell treatments, the mitochondrial membrane potential of SK-N-SH cells was detected using a JC-1 assay kit (cat. no. C2006; Beyotime Institute of Biotechnology) according to the manufacturer's instructions. Briefly, SK-N-SH cells were cultured in six-well plates at $3x10^5$/well for 24 h at 37˚C, followed by staining with JC-1 solution for 20 min at 37˚C in the dark. Finally, SK-N-SH cells were washed using PBS, before being imaged using a fluorescence microscope (Olympus Corp.) at an excitation wavelength of 488 nm and an emission wavelength of 525 nm to determine the fluorescence intensity.

Reverse transcription-quantitative PCR (RT-qPCR). Total RNA was extracted from SK-N-SH cells using the TRIzol® reagent (Thermo Fisher Scientific, Inc.), which was then converted to cDNA using PrimeScript™ RT Master Mix (Takara Biotechnology Co., Ltd.) according to the manufacturer's instructions. cDNA was then amplified by RT-qPCR using SYBR® Premix Ex Taq™ (Takara Biotechnology Co., Ltd.) in a 7500 Real-Time PCR System (Applied Biosystems; Thermo Fisher Scientific, Inc.). The following thermocycling conditions were used: Initial denaturation at 94˚C for 10 min,

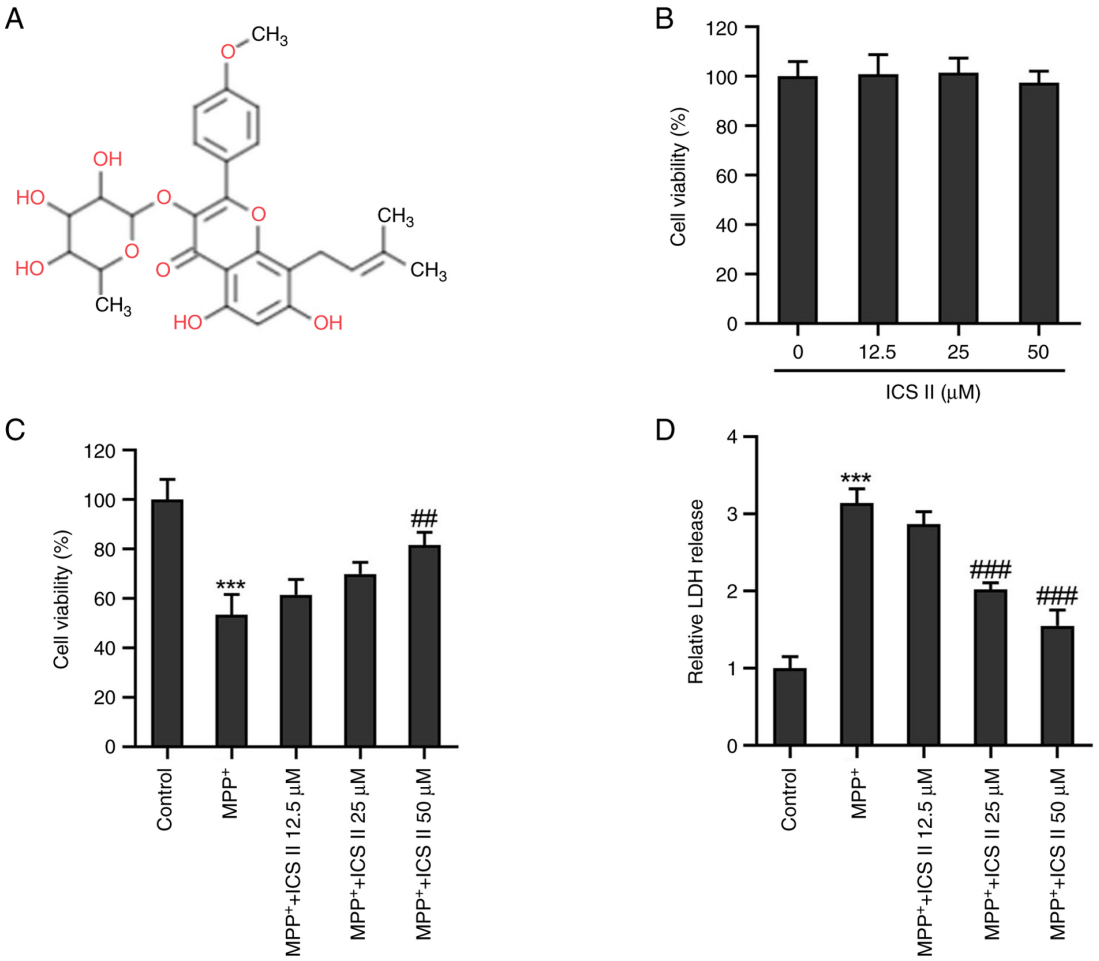

Figure 1. ICS II mitigates SK-N-SH cytotoxicity induced by MPP+. (A) ICS II chemical structure formula. (B) Viability of SK-N-SH cells treated with different concentrations of ICS II was determined by MTT assay. (C) Viability of MPP+-induced SK-N-SH cells treated with different concentrations of ICS II was determined by MTT assay. (D) LDH release of MPP+-induced SK-N-SH cells treated with different concentrations of ICS II was determined using an LDH activity assay kit. ***P<0.001 vs. Control; ##P<0.01 and ###P<0.001 vs. MPP+. ICS II, icariside II; MPP+, 1-methyl-4-phenylpyridinium; LDH, lactate dehydrogenase.

followed by 40 cycles at 94˚C for 10 sec, 60˚C for 20 sec and 72˚C for 1 min. The primer sequences used in the present study were as follows: HDAC2 forward (F), 5'-GCTATTCCAGAA GATGCTGTTC-3' and reverse (R), 5'-GTTGCTGAGCTG TTCTGATTTG-3'; and GAPDH F, 5'-CAGGAGGCATTG CTGATGAT-3' and R, 5'-GAAGGCTGGGGCTCATTT-3'. mRNA expression was quantified using the $2^{-\Delta\Delta Cq}$ method and normalized to GAPDH (20).

For the measurement of the mitochondrial DNA (mtDNA) content, total DNA extracted from SK-N-SH cells was purified using TIANamp Genomic DNA Kit (cat. no. DP304; Tiangen Biotech Co., Ltd.) according to the manufacturer's instructions. The relative mtDNA copy number was evaluated via qPCR amplification of the mitochondrial D-loop using SYBR® Premix Ex Taq™ (Takara Biotechnology Co., Ltd.) as mentioned above using the following primers: F, 5'-ATGGCC AACCTCCTACTCCT-3' and R, 5'-GCGGTGATGTAGAGG GTGAT-3', with GAPDH as a normalization control.

Detection of lactate dehydrogenase (LDH) release, ATP level and complex I activity. LDH release, ATP levels and Complex I activity of treated SK-N-SH cells seeded into 96-well plates at a density of $5x10^4$ cells/well were determined using the LDH Cytotoxicity Assay Kit (cat. no. C0016; Beyotime Institute of Biotechnology), ATP Assay Kit (cat. no. S0026; Beyotime Institute of Biotechnology) and Complex I Enzyme Activity Microplate Assay Kit (colorimetric; cat. no. ab109721; Abcam) according to the manufacturer's instructions.

Mitochondrial permeability transition pore (mPTP) opening evaluation. Cellular mPTP opening was measured using an mPTP Assay Kit (cat. no. C2009S; Beyotime Institute of Biotechnology) according to the manufacturer's instructions. SK-N-SH cells seeded in 24-well plates ($5x10^5$ cells/well) were stained using 5 μM Calcein AM reaction mixture (Santa Cruz Biotechnology, Inc.) for 30 min at 37˚C in the dark. After washing with PBS, the fluorescence intensity was observed using a fluorescence microscope (Olympus Corp.) at 490 nm for excitation and 515 nm for emission. The loss of calcein fluorescence in SK-N-SH cells indicated the opening of the mPTP.

Molecular docking. The crystal structure of HDAC2 [protein data bank (PDB) ID: 4LY1] was downloaded from the PDB website (http://www.rcsb.org/) and saved in PDB format. The 3D structure of ICS II was obtained from the PubChem

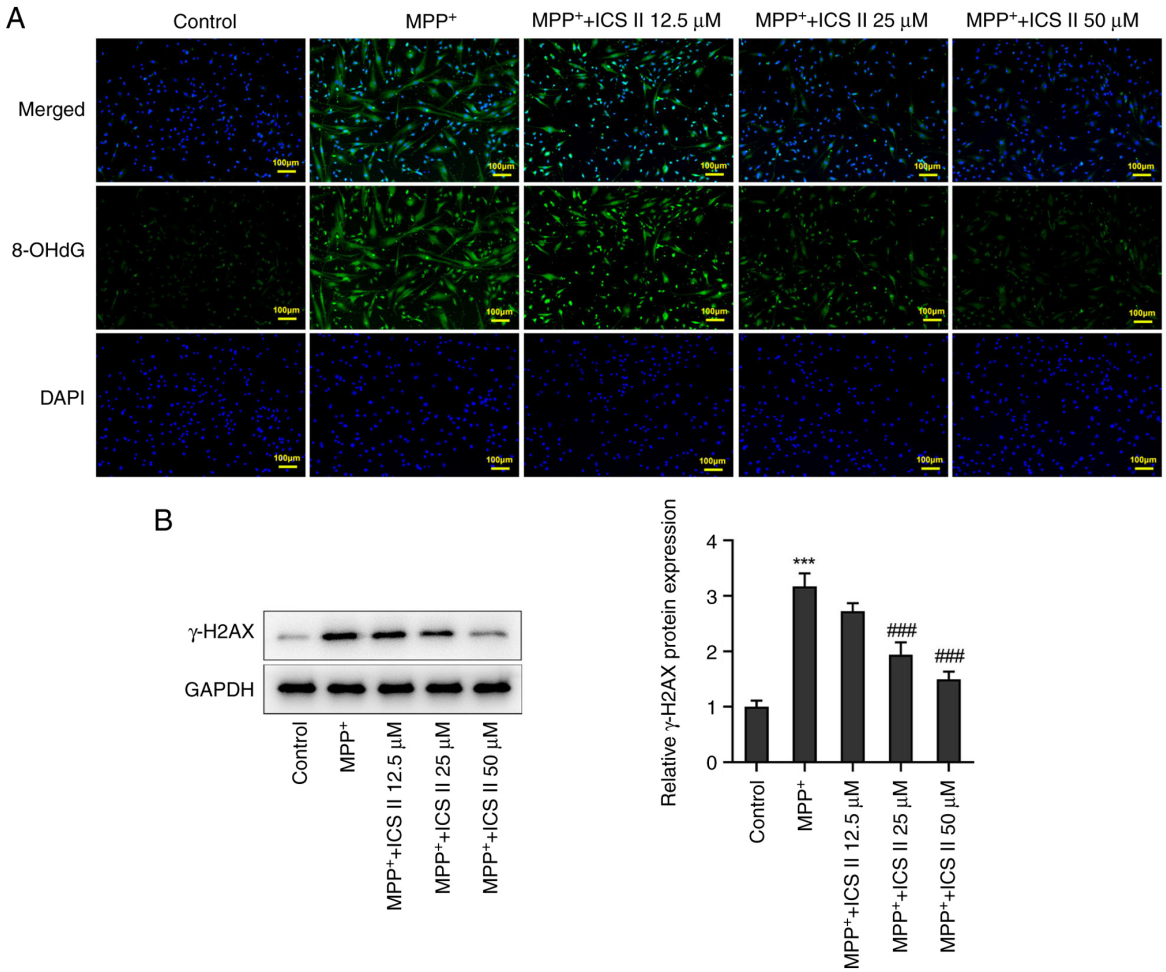

Figure 2. ICS II alleviates DNA damage in SK-N-SH cells induced by MPP+. (A) Production of 8-OHdG by MPP+-induced SK-N-SH cells treated with different concentrations of ICS II was detected by immunofluorescence (scale bars, 100 μm). (B) Protein expression levels of γ-H2AX in MPP+-induced SK-N-SH cells treated with different concentrations of ICS II were detected by western blotting. ***P<0.001 vs. Control; ###P<0.001 vs. MPP+. ICS II, icariside II; MPP+, 1-methyl-4-phenylpyridinium; 8-OHdG, 8-hydroxydesoxyguanosin; γ-H2AX, γ-H2A histone family member X.

database (https://pubchem.ncbi.nlm.nih.gov/compound/13964067#section=3D-Conformer). Molecular docking was used to predict the optimal binding site of ICS II to HDAC2 using AutoDock (version 4.2; Scripps Institute). The optimal binding mode between ICS II and HDAC2 was acquired under the minimum binding free energy conformation, before the output results were visualized in PyMOL (version 2.2.0) software (Schrödinger, LLC).

Statistical analysis. GraphPad Prism 8 (GraphPad Software; Dotmatics) was used to perform statistical analysis. The results are expressed as the mean ± standard deviation. One-way analysis of variance and Tukey's post-hoc test were used to compare differences among multiple groups. P<0.05 was considered to indicate a statistically significant difference.

Results

ICS II mitigates SK-N-SH cytotoxicity induced by MPP+. To explore the cytotoxicity of ICS II, SK-N-SH cells were treated with different concentrations (0, 12.5, 25 and 50 μM) of ICS II. The MTT assay demonstrated that the different concentrations of ICS II tested did not influence SK-N-SH cell viability (Fig. 1B), suggesting that ICS II was not harmful to SK-N-SH cells at the concentrations tested in the present study. By contrast, treatment with 2 mM MPP+ significantly decreased the viability of SK-N-SH cells compared with that in the control group, which was in turn significantly reversed by treatment with 50 μM ICS II (Fig. 1C). LDH release by MPP+-induced SK-N-SH cells was found to be significantly increased compared with that in the control group, but ICS II treatment (25 and 50 μM) significantly decreased the LDH release induced by MPP+ in SK-N-SH cells (Fig. 1D). These results suggest that ICS II restored the viability of SK-N-SH cells treated with MPP+.

ICS II alleviates DNA damage in SK-N-SH cells induced by MPP+. 8-OHdG is a marker of free radical-induced oxidative DNA lesions (21). MPP+ treatment caused a marked increase in the production of 8-OHdG in SK-N-SH cells compared with that in the control group, suggesting that MPP+ caused DNA damage in SK-N-SH cells. By contrast, ICS II reversed the production of 8-OHdG in MPP+-treated SK-N-SH cells in a dose-dependent manner (Fig. 2A). The protein expression level of γ-H2AX was also found to be significantly increased in MPP+-induced SK-N-SH cells compared with that in the

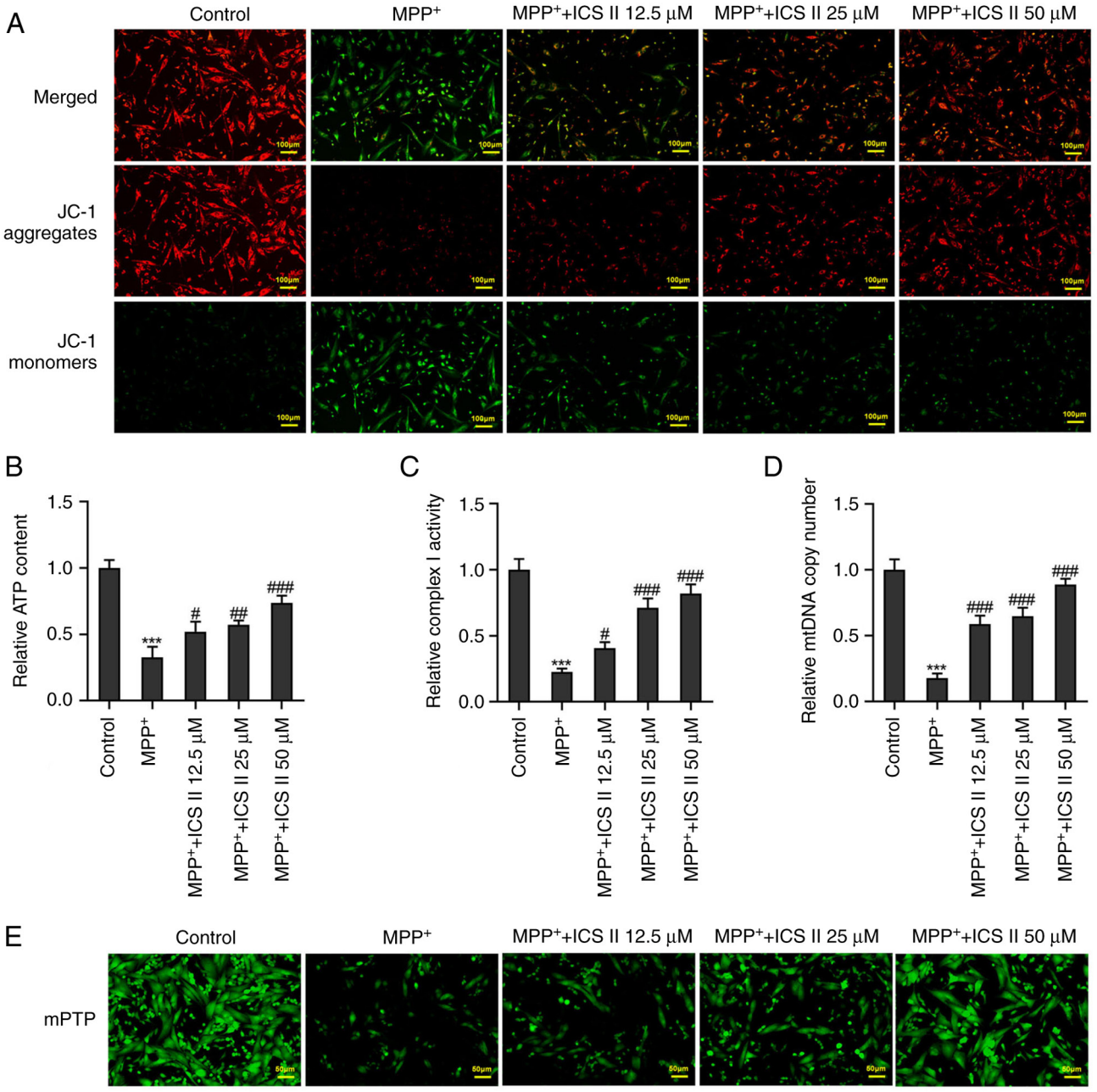

Figure 3. ICS II prevents MPP+-induced mitochondrial dysfunction in SK-N-SH cells. (A) The mitochondrial membrane potential of MPP^+-induced SK-N-SH cells treated by different concentrations of ICS II was detected by JC-1 staining (scale bars, 100 μm). (B) ATP content and (C) Complex I activity in MPP^+-induced SK-N-SH cells treated by different concentrations of ICS II was detected using ATP assay kit and Complex I assay kit, respectively. (D) mtDNA copy number in MPP^+-induced SK-N-SH cells treated by different concentrations of ICS II was detected by reverse transcription-quantitative PCR. (E) mPTP opening status in MPP^+-induced SK-N-SH cells was detected using the mPTP Assay Kit (scale bars, 50 μm). ***P<0.001 vs. Control; $^{\#}$P<0.05, $^{\#\#}$P<0.01 and $^{\#\#\#}$P<0.001 vs. MPP^+. ICS II, icariside II; MPP^+, 1-methyl-4-phenylpyridinium; mtDNA, mitochondrial DNA; mPTP, mitochondrial permeability transition pore.

control group, but this was in turn significantly reversed by 25 and 50 μM ICS II treatment (Fig. 2B). These results suggest that ICS II can protect against DNA damage in MPP^+-treated SK-N-SH cells.

ICS II reverses MPP^+-induced mitochondrial dysfunction in SK-N-SH cells. The JC-1 fluorescent probe, which has an excitation wavelength of 488 nm and a monomer emission wavelength of 525 nm, is able to enter cells and localize to the mitochondrial membrane (22). MPP^+ was observed to markedly decrease the mitochondrial membrane potential in SK-N-SH cells, which was reversed by ICS II treatment (Fig. 3A). The ATP content, complex I activity and mtDNA copy number were all significantly reduced by MPP^+ treatment in SK-N-SH cells compared with those in the control group (Fig. 3B-D). By contrast, ICS II treatment significantly increased the ATP content, Complex I activity and mtDNA copy number in MPP^+-treated SK-N-SH cells at all concentrations tested (Fig. 3B-D). There is an inverse correlation between the number of mPTP opening and the calcein-AM fluorescence intensity (23). ICS II treatment also markedly decreased mPTP opening in MPP^+-induced SK-N-SH cells

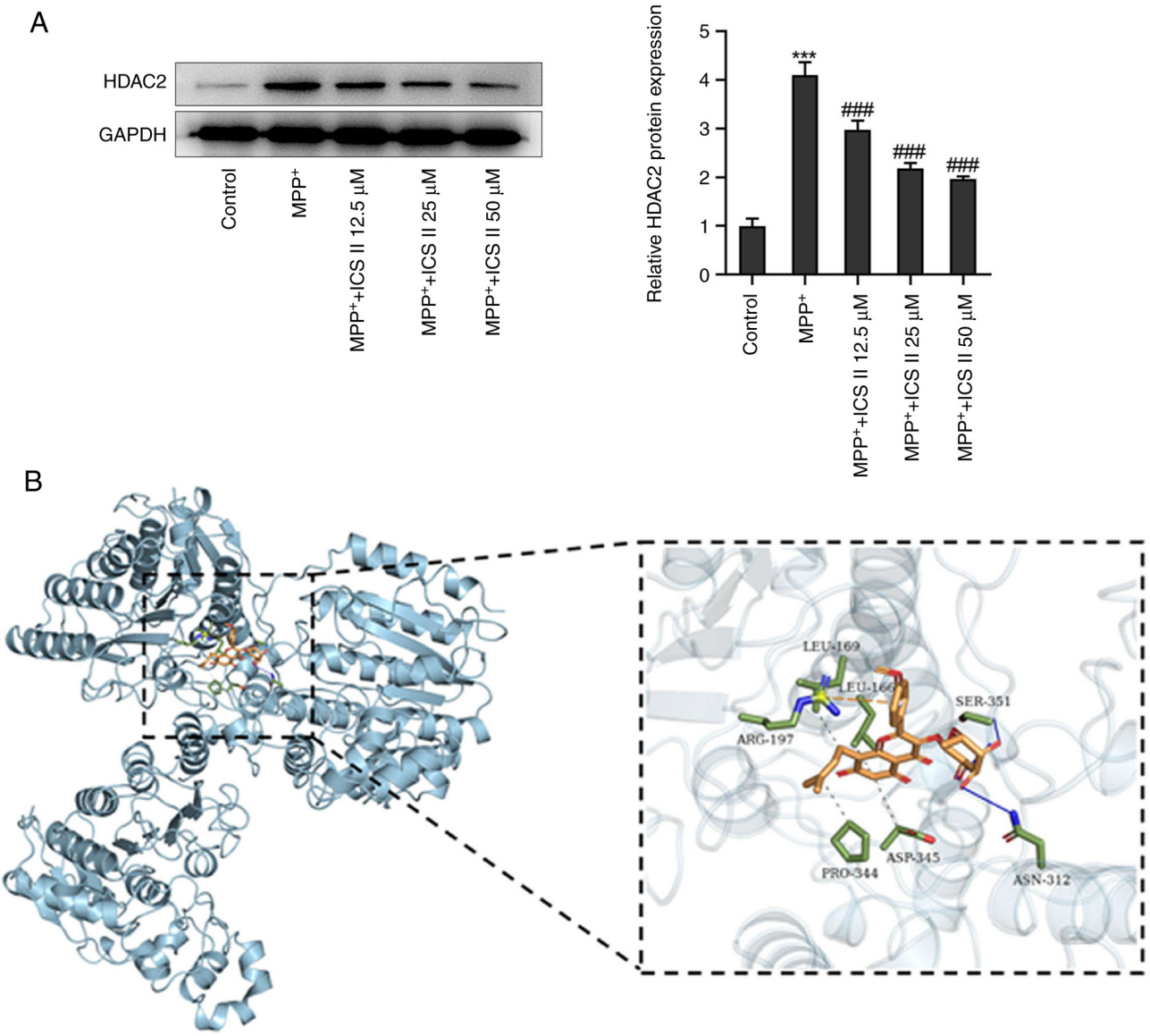

Figure 4. ICS II downregulates HDAC2 expression in MPP+-induced SK-N-SH cells. (A) Protein expression levels of HDAC2 in MPP+-induced SK-N-SH cells treated with different concentrations of ICS II were detected by western blotting. (B) Molecular docking was performed among HDAC2 and ICS II. ***P<0.001 vs. Control; ###P<0.001 vs. MPP+. ICS II, icariside II; MPP+, 1-methyl-4-phenylpyridinium; HDAC2, histone deacetylase 2.

in a dose-dependent manner (Fig. 3E). These results suggest that ICS II treatment can improve mitochondrial function in MPP+-treated SK-N-SH cells.

ICS II downregulates HDAC2 expression in MPP+-induced SK-N-SH cells. MPP+ was found to significantly increase the protein expression levels of HDAC2 in SK-N-SH cells, which was significantly reversed by ICS II at all concentrations tested (Fig. 4A). Molecular docking was then performed between HDAC2 and ICS II, where the position with the lowest free energy (-7.7 kcal/mol) between HDAC2 and ICS II was selected for visualization. The HDAC2/ICS II complex was found in the residues LEU-169, LEU-166, SER-351, ARG-197, PRO-344, ASP-345 and ASN-312. Of note, ICS II formed two hydrogen bonds, primarily with residues (SER-351 and ASN-312) on HDAC2 protein (Fig. 4B). Moreover, ICS II at the concentration of 50 μM exhibited the most prominent effect, thence being chosen for the subsequent assays. These results suggest that ICS II could bind to HDAC2 whilst also decreasing its protein expression levels.

Overexpression of HDAC2 reverses the protective effects of ICS II on MPP+-induced SK-N-SH cells. Transfection of SK-N-SH cells with Oe-HDAC2 was found to significantly increase the mRNA and protein expression levels of HDAC2 compared with those in the control group (Fig. 5A and B). In addition, HDAC2 overexpression significantly increased LDH release in MPP+-induced SK-N-SH cells treated with 50 μM ICS II compared with that in the cells transfected with Oe-NC (Fig. 5C). 8-OHdG production was also markedly increased upon the overexpression of HDAC2, compared with that in MPP+-induced and ICS II-treated SK-N-SH cells transfected with Oe-NC (Fig. 5D). Furthermore, protein expression levels of γ-H2AX in MPP+-induced SK-N-SH cells treated with ICS II were significantly increased by the overexpression of HDAC2 compared with cells transfected with Oe-NC (Fig. 5E).

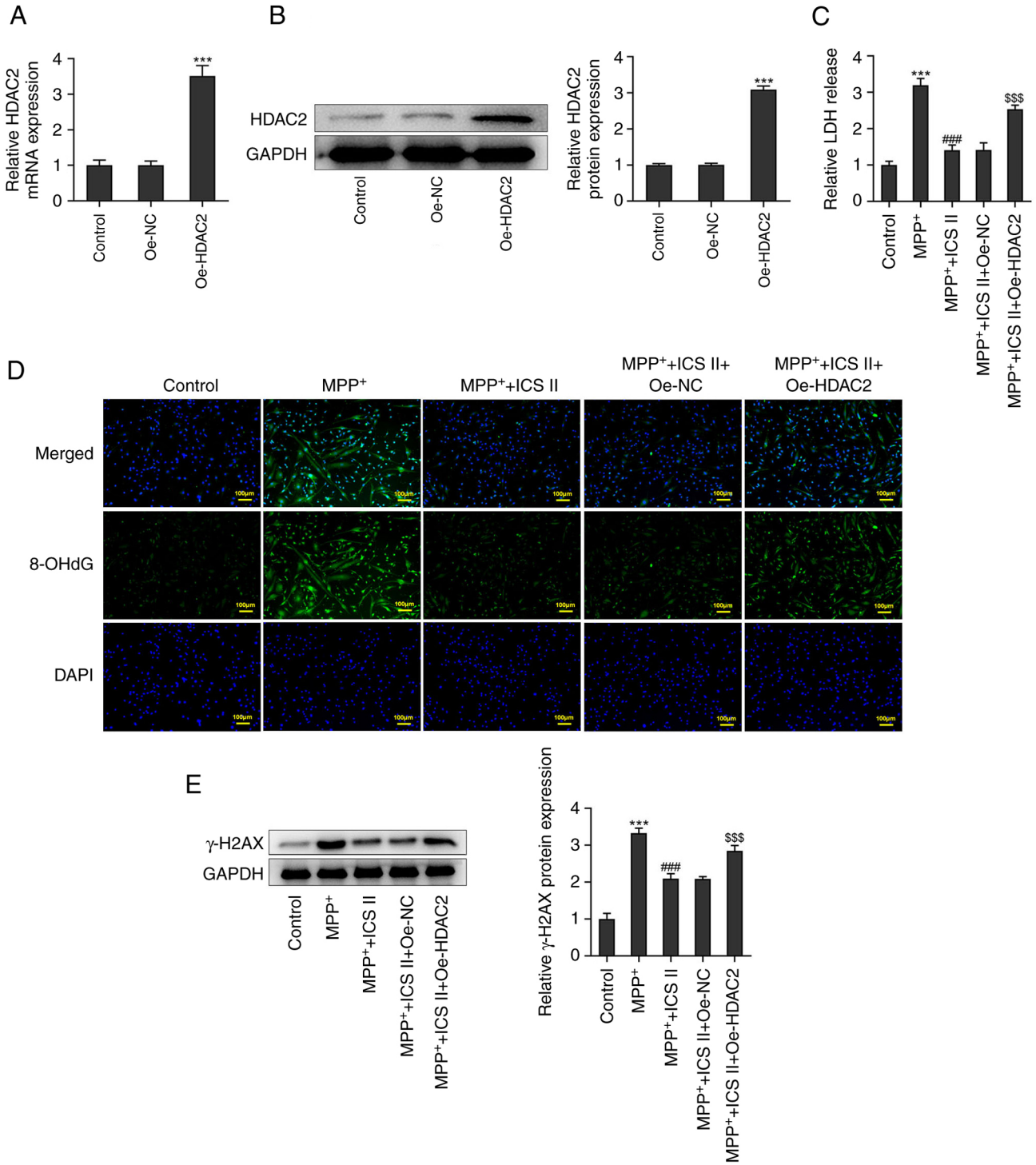

Figure 5. Overexpression of HDAC2 reverses the protective effects of ICS II on DNA damage in MPP^+-induced SK-N-SH cells. (A) mRNA and (B) protein expression levels of HDAC2 in SK-N-SH cells transfected with Oe-HDAC2 were detected by reverse transcription-quantitative PCR and western blotting, respectively. (C) LDH release of Oe-HDAC2-transfected SK-N-SH cells treated with MPP+ and ICS II was detected with an LDH activity assay kit. (D) Production of 8-OHdG by Oe-HDAC2-transfected SK-N-SH cells treated with MPP+ and ICS II was detected by immunofluorescence (scale bars, 100 μm). (E) Protein expression levels of γ-H2AX in Oe-HDAC2-transfected SK-N-SH cells treated with MPP+ and ICS II were detected by western blotting. ***P<0.001 vs. Control; $^{###}$P<0.001 vs. MPP^+; $^{\$\$\$}$P<0.001 vs. MPP^+ + ICS II + Oe-NC. ICS II, icariside II; MPP+, 1-methyl-4-phenylpyridinium; 8-OHdG, 8-hydroxydesoxyguanosin; γ-H2AX, γ-H2A histone family member X; HDAC2, histone deacetylase 2; Oe, overexpression; NC, negative control; LDH, lactate dehydrogenase.

HDAC2 overexpression also markedly decreased the mitochondrial membrane potential in MPP^+-induced SK-N-SH cells treated with ICS II compared with that in cells transfected with Oe-NC (Fig. 6A). Additionally, HDAC2 overexpression significantly decreased the ATP content, complex I activity and the mtDNA copy number in MPP^+-induced SK-N-SH cells treated with ICS II compared with those in cells transfected with Oe-NC (Fig. 6B-D). HDAC2 overexpression also markedly increased mPTP opening in MPP^+-induced SK-N-SH cells treated with ICS II compared with that in cells transfected with

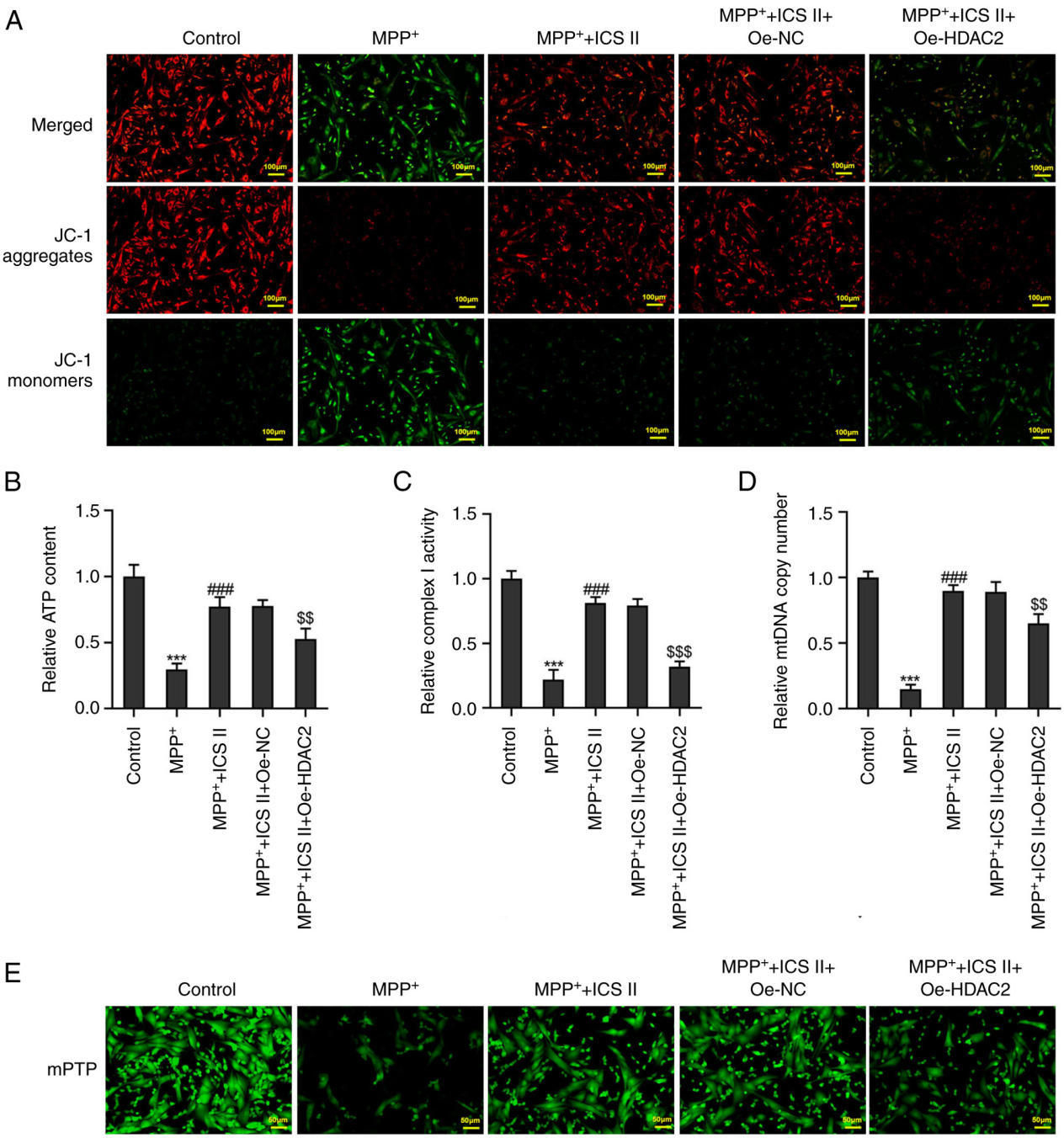

Figure 6. Overexpression of HDAC2 reverses the protective effects of ICS II against mitochondrial dysfunction in MPP+-induced SK-N-SH cells. (A) Mitochondrial membrane potential of Oe-HDAC2-transfected SK-N-SH cells treated with MPP+ and ICS II was detected using JC-1 staining (scale bars, 100 μm). (B) ATP content of Oe-HDAC2-transfected SK-N-SH cells treated with MPP+ and ICS II was determined using an ATP assay kit. (C) Complex I activity in Oe-HDAC2-transfected SK-N-SH cells treated with MPP+ and ICS II was detected using Complex I assay kit. (D) mtDNA copy number in Oe-HDAC2-transfected SK-N-SH cells treated with MPP+ and ICS II was determined using reverse transcription-quantitative PCR. (E) mPTP opening status in Oe-HDAC2-transfected SK-N-SH cells treated with MPP+ and ICS II was detected using a mPTP Assay Kit (scale bars, 50 μm). ***P<0.001 vs. Control; $^{###}$P<0.001 vs. MPP+; $^{\$\$}$P<0.01 and $^{\$\$\$}$P<0.001 vs. MPP+ + ICS II + Oe-NC. ICS II, icariside II; MPP+, 1-methyl-4-phenylpyridinium; mtDNA, mitochondrial DNA; mPTP, mitochondrial permeability transition pore; HDAC2, histone deacetylase 2; Oe, overexpression; NC, negative control.

Oe-NC (Fig. 6E). These results suggest that HDAC2 overexpression promoted DNA damage and mitochondrial dysfunction in MPP+-induced SK-N-SH cells treated with ICS II.

Discussion

In the present study, the effect of ICS II on DNA damage and mitochondrial function in MPP+-induced SK-N-SH cells was investigated. It was demonstrated that ICS II can increase cell viability whilst alleviating DNA damage and mitochondrial dysfunction in MPP+-induced SK-N-SH cells. ICS II treatment was found to inhibit the expression of HDAC2, whilst HDAC2 overexpression could reverse the effects of ICS II treatment on SK-N-SH cells. These findings suggest that ICS II can be used as a potentially promising future treatment method for PD.

Mitochondrial homeostasis is necessary for generating energy in the form of ATP, regulating calcium homeostasis and controlling programmed cell death (24). Imbalance in mitochondrial homeostasis can lead to the development of progressive pathological conditions, including Alzheimer's disease, Parkinson's disease (PD), Huntington's disease and amyotrophic lateral sclerosis, associated with aging and neurodegeneration (25,26). In particular, mitochondrial dysfunction serves a key role in the development of PD. In patients with PD, mitochondrial respiratory chain complex I activity is decreased and reactive oxygen species (ROS) production is increased, which leads to the depolarization of the mitochondrial membrane potential and the increase in membrane permeability, ultimately causing membrane damage (27). The present study demonstrated that MPP^+ induction was able to decrease the mitochondrial membrane potential, reduce the intracellular ATP content and complex I activity whilst increasing mPTP opening in SK-N-SH cells.

mPTP-induced inflammation and dopaminergic neuronal death can be alleviated by improving mitochondrial function (28). A previous study involving an *in vivo* PD model of MPP^+/mPTP-induced SH-SY5Y cells reported that MPP^+-induced mitochondrial damage can be reversed by promoting mitophagy and suppressing mitochondrial fission (29). HDAC2 inhibition may suppress the mitochondrial apoptosis pathway to protect against acute liver failure (16,30). In another study, blocking HDAC2 was found to improve neuronal mitochondrial dynamics to protect neurons against oxidative injury and apoptosis (31). ICS II has previously been reported to inhibit mitochondrial division in the hippocampus of $A\beta_{25-35}$-induced rats (9). ICS II has also been shown to prevent myocardial infarction-induced mitochondrial oxidative stress (32). In PC12 cells that had underwent oxygen-glucose deprivation and reoxygenation, ICS II was found to restore the mitochondrial membrane potential by suppressing the excessive production of mitochondrial ROS (33). The present study demonstrated that HDAC2 was a potential target of ICS II using SuperPreD database and provided evidence that ICS II treatment downregulated HDAC2 expression in MPP^+-induced SK-N-SH cells. In addition, ICS II was observed to alleviate DNA damage and restored mitochondrial function in MPP^+-induced SK-N-SH cells by decreasing HDAC2 expression. Furthermore, rescue experiments were performed to confirm whether ICS II exerted its protective effects on MPP^+-induced SK-N-SH cells through HDAC2. HDAC2 overexpression was found to negate the protective effect of ICS II on MPP^+-induced SK-N-SH cells, suggesting that ICS II can protect SK-N-SH cells from MPP^+-induced DNA damage and mitochondrial dysfunction by downregulating HDAC2 expression.

In conclusion, the present study demonstrated that ICS II exerts a protective role against MPP^+-induced neurotoxicity, where HDAC2 is a potential target of ICS II. Therefore, ICS II or alternative treatment strategies to reduce the expression of HDAC2 may provide novel therapeutic options for restoring mitochondrial function in dopaminergic neurons for the treatment of PD.

Acknowledgements

Not applicable.

Funding

No funding was received.

Availability of data and materials

The datasets used and/or analyzed during the current study are available from the corresponding author on reasonable request.

Authors' contributions

WF and JZ designed the study, performed the experiments and drafted and revised the manuscript. WF analyzed the data and searched the literature. Both authors read and approved the final version of the manuscript. WF and JZ confirm the authenticity of all the raw data.

Ethics approval and consent to participate

Not applicable.

Patient consent for publication

Not applicable.

Competing interests

The authors declare that they have no competing interests.

References

1. Sharma S, Awasthi A and Singh S: Altered gut microbiota and intestinal permeability in Parkinson's disease: Pathological highlight to management. Neurosci Lett 712: 134516, 2019.
2. Nair AT, Ramachandran V, Joghee NM, Antony S and Ramalingam G: Gut microbiota dysfunction as reliable non-invasive early diagnostic biomarkers in the pathophysiology of Parkinson's disease: A critical review. J Neurogastroenterol Motil 24: 30-42, 2018.
3. Xu X, Wang R, Hao Z, Wang G, Mu C, Ding J, Sun W and Ren H: DJ-1 regulates tyrosine hydroxylase expression through CaMKKβ/CaMKIV/CREB1 pathway in vitro and in vivo. J Cell Physiol 235: 869-879, 2020.
4. Yin C, Deng Y, Liu Y, Gao J, Yan L and Gong Q: Icariside II ameliorates cognitive impairments induced by chronic cerebral hypoperfusion by inhibiting the amyloidogenic pathway: Involvement of BDNF/TrkB/CREB signaling and up-regulation of PPARα and PPARγ in rats. Front Pharmacol 9: 1211, 2018.
5. Deng Y, Xiong D, Yin C, Liu B, Shi J and Gong Q: Icariside II protects against cerebral ischemia-reperfusion injury in rats via nuclear factor-κB inhibition and peroxisome proliferator-activated receptor up-regulation. Neurochem Int 96: 56-61, 2016.
6. Yan BY, Pan CS, Mao XW, Yang L, Liu YY, Yan L, Mu HN, Wang CS, Sun K, Liao FL, *et al*: Icariside II improves cerebral microcirculatory disturbance and alleviates hippocampal injury in gerbils after ischemia-reperfusion. Brain Res 1573: 63-73, 2014.
7. Yin C, Deng Y, Gao J, Li X, Liu Y and Gong Q: Icariside II, a novel phosphodiesterase-5 inhibitor, attenuates streptozotocin-induced cognitive deficits in rats. Neuroscience 328: 69-79, 2016.
8. Deng Y, Long L, Wang K, Zhou J, Zeng L, He L and Gong Q: Icariside II, a broad-spectrum anti-cancer agent, reverses beta-amyloid-induced cognitive impairment through reducing inflammation and apoptosis in rats. Front Pharmacol 8: 39, 2017.
9. Xiao HH, Chen JC, Li H, Li RH, Wang HB, Song HP, Li HY, Shan GS, Tian Y, Zhao YM, *et al*: Icarisid II rescues cognitive dysfunction via activation of Wnt/β-catenin signaling pathway promoting hippocampal neurogenesis in APP/PS1 transgenic mice. Phytother Res 36: 2095-2108, 2022.

10. Yan L, Deng Y, Gao J, Liu Y, Li F, Shi J and Gong Q: Icariside II effectively reduces spatial learning and memory impairments in Alzheimer's disease model mice targeting beta-amyloid production. Front Pharmacol 8: 106, 2017.
11. Li Y, Gu Z, Lin S, Chen L, Dzreyan V, Eid M, Demyanenko S and He B: Histone deacetylases as epigenetic targets for treating Parkinson's disease. Brain Sci 12: 672, 2022.
12. Ma P and Schultz RM: HDAC1 and HDAC2 in mouse oocytes and preimplantation embryos: Specificity versus compensation. Cell Death Differ 23:1119-1127, 2016.
13. Stoddard SV, May XA, Rivas F, Dodson K, Vijayan S, Adhika S, Parker K and Watkins DL: Design of potent panobinostat histone deacetylase inhibitor derivatives: Molecular considerations for enhanced isozyme selectivity between HDAC2 and HDAC8. Mol Inform 38: e1800080, 2019.
14. Chen J, Li N, Liu B, Ling J, Yang W, Pang X and Li T: Pracinostat (SB939), a histone deacetylase inhibitor, suppresses breast cancer metastasis and growth by inactivating the IL-6/STAT3 signalling pathways. Life Sci 248: 117469, 2020.
15. Tan Y, Delvaux E, Nolz J, Coleman PD, Chen S and Mastroeni D: Upregulation of histone deacetylase 2 in laser capture nigral microglia in Parkinson's disease. Neurobiol Aging 68: 134-141, 2018.
16. Choong CJ, Sasaki T, Hayakawa H, Yasuda T, Baba K, Hirata Y, Uesato S and Mochizuki H: A novel histone deacetylase 1 and 2 isoform-specific inhibitor alleviates experimental Parkinson's disease. Neurobiol Aging 37: 103-116, 2016.
17. Singer TP and Ramsay RR: Mechanism of the neurotoxicity of MPTP. An update. FEBS Lett 274: 1-8, 1990.
18. Yuan X, Wu Y, Lu L and Feng J: Long noncoding RNA SNHG14 knockdown exerts a neuroprotective role in MPP+-induced Parkinson's disease cell model through mediating miR-135b-5p/KPNA4 axis. Metab Brain Dis 37: 2363-2373, 2022.
19. Xu F, Lv C, Deng Y, Liu Y, Gong Q, Shi J and Gao J: Icariside II, a PDE5 inhibitor, suppresses oxygen-glucose deprivation/reperfusion-induced primary hippocampal neuronal death through activating the PKG/CREB/BDNF/TrkB signaling pathway. Front Pharmacol 11: 523, 2020.
20. Livak KJ and Schmittgen TD: Analysis of relative gene expression data using real-time quantitative PCR and the 2(-Delta Delta C(T)) method. Methods 25: 402-408, 2001.
21. Halczuk KM, Boguszewska K, Urbaniak SK, Szewczuk M and Karwowski BT: 8-oxo-7,8-dihydro-2'-deoxyguanosine (8-oxodG) and 8-hydroxy-2'-deoxyguanosine (8-OHdG) as a cause of autoimmune thyroid diseases (AITD) during pregnancy? Yale J Biol Med 93: 501-515, 2020.
22. Perelman A, Wachtel C, Cohen M, Haupt S, Shapiro H and Tzur A: JC-1: Alternative excitation wavelengths facilitate mitochondrial membrane potential cytometry. Cell Death Dis 3: e430, 2012.
23. Jiang DQ, Ma YJ, Wang Y, Lu HX, Mao SH and Zhao SH: Microglia activation induces oxidative injury and decreases SIRT3 expression in dopaminergic neuronal cells. J Neural Transm (Vienna) 126:559-568, 2019.
24. Harrington JS, Ryter SW, Plataki M, Price DR and Choi AMK: Mitochondria in health, disease, and aging. Physiol Rev 103: 2349-2422, 2023.
25. Golpich M, Amini E, Mohamed Z, Azman Ali R, Mohamed Ibrahim N and Ahmadiani A: Mitochondrial dysfunction and biogenesis in neurodegenerative diseases: Pathogenesis and treatment. CNS Neurosci Ther 23: 5-22, 2017.
26. Grimm A and Eckert A: Brain aging and neurodegeneration: From a mitochondrial point of view. J Neurochem 143: 418-431, 2017.
27. Park JS, Davis RL and Sue CM: Mitochondrial dysfunction in Parkinson's disease: New mechanistic insights and therapeutic perspectives. Curr Neurol Neurosci Rep 18: 21, 2018.
28. Kim HY, Bae CH, Kim J, Lee Y, Jeon H, Kim H and Kim S: Rumex japonicus houtt. protects dopaminergic neurons by regulating mitochondrial function and gut-brain axis in in vitro and in vivo models of Parkinson's disease. Antioxidants (Basel) 11: 141, 2022.
29. Wu LK, Agarwal S, Kuo CH, Kung YL, Day CH, Lin PY, Lin SZ, Hsieh DJ, Huang CY and Chiang CY: Artemisia leaf extract protects against neuron toxicity by TRPML1 activation and promoting autophagy/mitophagy clearance in both in vitro and in vivo models of MPP+/MPTP-induced Parkinson's disease. Phytomedicine 104: 154250, 2022.
30. Liu Y, Wang Y, Chen Q, Jiao F, Wang L and Gong Z: HDAC2 inhibitor CAY10683 reduces intestinal epithelial cell apoptosis by inhibiting mitochondrial apoptosis pathway in acute liver failure. Histol Histopathol 34: 1173-1184, 2019.
31. Frankowski H, Yeboah F, Berry BJ, Kinoshita C, Lee M, Evitts K, Davis J, Kinoshita Y, Morrison RS and Young JE: Knock-down of HDAC2 in human induced pluripotent stem cell derived neurons improves neuronal mitochondrial dynamics, neuronal maturation and reduces amyloid beta peptides. Int J Mol Sci 22: 2526, 2021.
32. Li Y, Feng L, Xie D, Lin M, Li Y, Chen N, Yang D, Gao J, Zhu Y and Gong Q: Icariside II, a naturally occurring SIRT3 agonist, protects against myocardial infarction through the AMPK/PGC-1α/apoptosis signaling pathway. Antioxidants (Basel) 11: 1465, 2022.
33. Feng L, Gao J, Liu Y, Shi J and Gong Q: Icariside II alleviates oxygen-glucose deprivation and reoxygenation-induced PC12 cell oxidative injury by activating Nrf2/SIRT3 signaling pathway. Biomed Pharmacother 103: 9-17, 2018.